analytical chemistry

Article

pubs.acs.org/ac

Cavity-Enhanced Raman Spectroscopy in the Biosciences: In Situ, Multicomponent, and Isotope Selective Gas Measurements To Study Hydrogen Production and Consumption by *Escherichia coli*

Thomas W. Smith and Michael Hippler*

Department of Chemistry, University of Sheffield, Sheffield S3 7HF, United Kingdom

Supporting Information

ABSTRACT: Recently we introduced cavity-enhanced Raman spectroscopy (CERS) with optical feedback cw-diode lasers as a sensitive analytical tool. Here we report improvements made on the technique and its first application in the biosciences for in situ, multicomponent, and isotope selective gas measurements to study hydrogen production and consumption by *Escherichia coli*. Under anaerobic conditions, cultures grown on rich media supplemented with D-glucose or glycerol produce H_2 and simultaneously consume some of it. By introducing D_2 in the headspace, hydrogen production and consumption could be separated due to the distinct spectroscopic signatures of isotopomers. Different phases with distinctly different kinetic regimes of H_2 and CO_2 production and D_2 consumption were identified. Some of the D_2 consumed is converted back to H_2 via H/D exchange with the solvent. HD was formed only as a minor component. This reflects either that H/D exchange at hydrogenase active sites is rapid compared to the rate of recombination, rapid recapture of HD occurs after the molecule is formed, or that the active sites where D_2 oxidation and proton reduction occur are physically separated. Whereas in glucose supplemented cultures, addition of D_2 led to an increase in H_2 produced, while the yield of CO_2 remained unchanged; with glycerol, addition of D_2 led not only to increased yields of H_2, but also significantly increased CO_2 production, reflecting an impact on fermentation pathways. Addition of CO was found to completely inhibit H_2 production and significantly reduce D_2 oxidation, indicating at least some role for O_2-tolerant Hyd-1 in D_2 consumption.

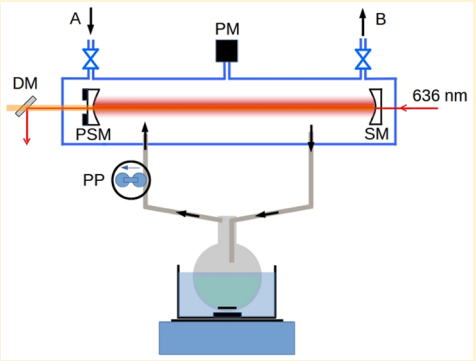

With concerns about greenhouse gas emissions and diminishing supplies of fossil fuels, focus is turning to renewable, net carbon-neutral sources of energy. Among these, dihydrogen (H_2) holds promise as a possible alternative, although there still remain challenges that must be overcome before a large-scale "Hydrogen Economy" could be feasible, including efficient storage, distribution, and improvements in sustainable production.[1−4] Biologically derived "biohydrogen" is a promising alternative to abiotic H_2 production.[5−7] Many microorganisms can produce H_2 either from breakdown of organic substrates or via light-driven processes.[8,9] The vast majority of microbial H_2 is generated by hydrogenases (see ref 10 for a recent review). Despite utilizing comparatively "poor", non-noble metals, hydrogenases achieve very high activities while operating under the relatively mild conditions of the intracellular environment. Unfortunately, most hydrogenases are sensitive to O_2.[7,10] Any industrial scale biohydrogen reactor would therefore require systems to monitor levels of O_2, to ensure efficient H_2 production and for safe operation. Simultaneous measurements of CO_2 and H_2 could also provide information on the metabolic condition of the culture and confirm that H_2 is produced at a satisfactory rate. Multicomponent gas measurements could also give mechanistic insights into these biological processes, aiding their optimization to maximize H_2 yields. Common analytical techniques include gas chromatography (GC) or mass spectrometry (MS); while sensitive and selective, they require expensive equipment and have limitations, including difficulties detecting certain components, long analysis times for GC, and the need for sample preparation, which prevents real-time, in situ monitoring.

Spectroscopic techniques are nonintrusive and provide data in real time for in situ monitoring with high selectivity and sensitivity, including the distinction of isotopomers.[11−25] Direct absorption techniques, like FTIR spectroscopy, are widely used but are unable to detect molecules such as H_2, O_2, or N_2. Due to different selection rules, Raman spectroscopy can monitor all relevant components.[16−25] Despite this, Raman scattering has not found widespread use in trace gas analysis due to its inherent weakness. Trace gas Raman spectroscopy at ambient pressures typically requires the use of large, high power laser systems or sophisticated equipment, which makes it difficult to use as analytical methods. Methods to increase sensitivity include stimulated Raman techniques such as PARS (Photoacoustic Stimulated Raman Spectroscopy) and CARS (Coher-

Received: December 11, 2016
Accepted: January 10, 2017
Published: January 10, 2017

DOI: 10.1021/acs.analchem.6b04924
Anal. Chem. 2017, 89, 2147−2154

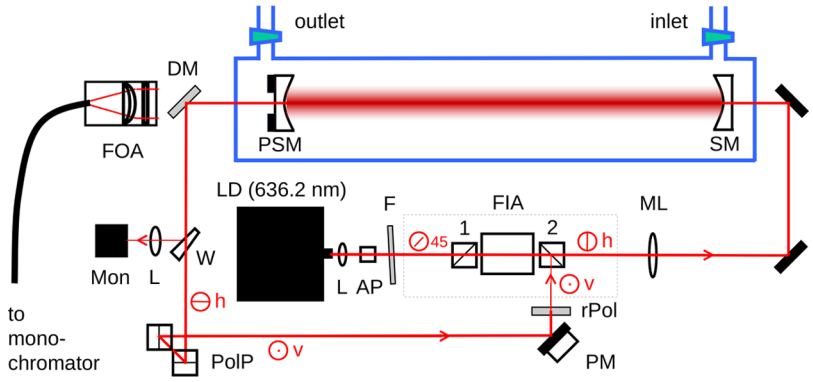

Figure 1. Scheme of the experimental setup (see main text for details).

ent Anti-Stokes Raman Spectroscopy), as well as Fiber-enhanced or cavity-enhanced Raman spectroscopy.[18−25]

Recently, we introduced cavity-enhanced Raman spectroscopy with optical feedback diode lasers (CERS), where an inexpensive diode laser is coupled into a high-finesse optical cavity, leading to power enhancement of about 3 orders of magnitude.[22,23] CERS has high spectral resolution due to the narrow laser line width obtained by controlled optical feedback. With a monochromator of sufficient spectral bandwidth, CERS can collect information on multiple components in a single acquisition. Here we describe the first application of CERS to the analysis of biohydrogen production from pure cultures. To demonstrate the utility of CERS for biohydrogen detection, we chose H_2-producing *Escherichia coli* (*E. coli*) as this model organism is well understood from a genetic and biochemical viewpoint, is easy to grow, and is reasonably amenable to genetic modification needed to improve H_2 yields.[26−28]

In the first section, the experimental apparatus and operating principles of CERS are outlined, and advancements made on this technique are described. We then report the application of CERS to the in situ headspace analysis of anaerobic batch cultures of *E. coli* supplemented with D-glucose or glycerol. We show how the kinetics of hydrogen uptake and formation reactions can be followed simultaneously by isotopically labeling the headspace above the culture. Finally, we demonstrate the ability of CERS to identify CO in the gas feed, a potent inhibitor for both H_2 producing hydrogenases and many proposed H_2 fuel cell technologies, and its effects on hydrogenase activity in whole *E. coli* cells.

EXPERIMENTAL SECTION

The principle of CERS with optical feedback has been described before,[22,23] but the current set up contains important improvements. Briefly, 10 mW laser radiation from a cw-laser diode **LD** at 636.18 nm (Hitachi HL6322G) is coupled via lens **L**, anamorphic prism pair **AP**, short-pass filter **F**, and mode matching lens **ML** into an optical cavity composed of two highly reflective mirrors (Newport SuperMirrors, $R > 99.99\%$) **SM** and **PSM** (Figure 1). Unwanted back reflections into the laser are prevented by a Faraday rotator isolator assembly, **FIA**. In previous implementations, two Faraday isolators were used in series to provide good isolation. In the meantime, we have found that one isolator is sufficient if it is carefully tuned for optimal isolation. If the laser wavelength matches the cavity length, an optical resonance builds up laser power inside the cavity by up to 3 orders of magnitude, which greatly increases Raman signals. After the cavity, a dichroic mirror **DM** separates excitation light from Raman signals, which are coupled into a fiber and transferred to the monochromator (Shamrock SR-750-A, with Andor iVac DR32400 camera at −60 °C). Part of the laser light is diverted back to the diode for optical feedback via the polarizing beam splitting cube **2** of **FIA**, locking the laser to the cavity; the intensity of the fed-back light can be adjusted via a rotating polarizer, **rPol**. The diode laser itself is linearly polarized at an angle of +45° to the optical bench. Polarizer **1** of **FIA** lets this component pass. The Faraday rotator rotates the polarization plane by −45°, so that afterward, the light is horizontally polarized with respect to the bench (0°) and passes polarizer **2**. The light exiting the optical cavity will also be mainly horizontally polarized, but this would make it unsuitable for optical feedback because, in the return path, polarizer **2** of **FIA** will only reflect vertically polarized light back to the diode. It is therefore necessary to rotate the polarization plane. This can be achieved by two mirrors or prisms (**PolP** in Figure 1), which first divert the beam by 90° up vertically from the bench and then immediately by 90° horizontally to the right of Figure 1, changing horizontal into vertical polarization. The light can then enter the Faraday rotator via polarizing beam splitting cube **2**, where it will be optically rotated by −45° to become +45°, which can pass polarizer **1** to feed back into the diode. **PolP** is essential if the set up uses one Faraday rotator.

The diode injection current is modulated around one cavity mode; in each cycle, the wavelength changes until it is locked to a longitudinal mode of the cavity by optical feedback. Previously, electronic locking circuits and mirrors mounted on piezoelectric transducers (**PSM** and **PM** in Figure 1) were used for mode and phase matching.[22,23] In a significant simplification, we have found that with sufficiently strong optical feedback, the laser will effectively self-lock and electronic mode tracking is not essential. Although resonances are less regular, Raman intensity fluctuations can be very effectively normalized using the N_2 Raman peak as an internal standard, if N_2 remains constant in the system. At 30 s acquisition time, noise-equivalent detection limits are about 0.14 mbar H_2 using a high-resolution grating (0.8 cm^{-1} resolution, 500 cm^{-1} spectral range),[22,23] and 1 mbar H_2 with a low-resolution grating (12 cm^{-1} resolution, 4000 cm^{-1} spectral range). Detection limits, sensitivities, and relative intensities are discussed in detail in our previous publications;[22,23] for convenience, we include a summary in the Supporting Information (Table S1). Typical Raman spectra with the low resolution grating are shown in Figure 2 (see further below for details of this experiment). Raman intensity is converted to partial pressure using tabulated integrated areas

DOI: 10.1021/acs.analchem.6b04924
Anal. Chem. 2017, 89, 2147−2154

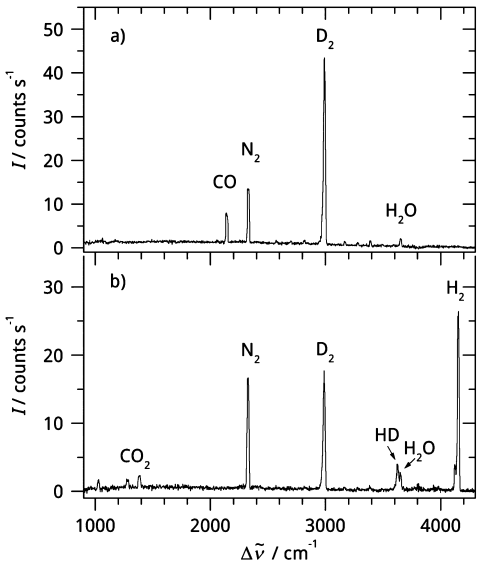

Figure 2. Typical CERS Raman spectra of the culture headspace in the anaerobic fermentation of 98 mM glycerol under an $N_2/D_2/CO$ atmosphere, (a) observed in the first phase after 76 min with CO, N_2, and D_2 present; (b) observed at the end of the second phase, where the CO was removed.

(Table S1).[23] At equilibrium, the molarity of a dissolved gas can be calculated from its partial pressure using Henry's law.[29] A small proportion of dissolved CO_2 will react with water to form carbonic acid, which will be at equilibrium with bicarbonate and carbonate ions, depending on the pH. With a typical acidic pH below 5 at the end of a fermentation experiment, less than 1% of dissolved CO_2 will be lost to carbonic acid and carbonates. The optical cavity is inside a vacuum-tight glass enclosure. Gas inlet and outlet taps allow controlled filling with gas mixtures. To characterize hydrogen leaking, CERS measurements of 1 bar mixtures of $H_2/D_2/N_2$ gave a loss rate of H_2 and D_2, with a half time of about 22−26 days, with H_2 on the lower end of this range and D_2 on the higher end.

E. coli (strain K-12 MG1655) was transferred from glycerol stock (maintained at −80 °C) and streaked on sterile LB-agar plates (LB, lysogeny broth, a nutrient rich growth medium). Plates were left overnight at 37 °C to allow distinct colonies to grow. For each measurement, 50 mL of sterile LB was inoculated with a single colony and grown anaerobically in a sealed 50 mL centrifuge tube for 16 h (37 °C, 200 rpm). The culture was added to 200 mL of fresh, sterile LB ($OD_{600} \approx 0.2$, optical density at 600 nm in a 1 cm cuvette), supplemented with either D-glucose or glycerol and transferred to the CERS apparatus. Bacterial suspensions were kept in the dark with constant stirring at 37 °C in a 500 mL round-bottom flask in a thermostated water bath. The flask was connected to the CERS enclosure with short gas transfer tubes, giving a total gas volume of 1330 mL. The transfer tubes and enclosure were kept at about 45 °C by a thermostated water jacket to avoid condensation. To enhance gas flow, a peristaltic pump (7 l/h) was used to cycle the flask headspace through the CERS vessel. In a test to characterize the experimental time resolution, CO_2 was generated from dry ice added to the flask normally used for biological measurements. The appearance time of CO_2 Raman signals in the CERS cell has a half time of about 2.5 min. At the beginning of an experiment, the system was repeatedly evacuated and then flushed with N_2 to remove O_2 before being filled with N_2, N_2/D_2, or $N_2/D_2/CO$ gas mixtures to a total pressure of 1 bar. During fermentation, CO_2 and H_2 were generated, increasing the pressure. At the end of a CERS measurement, the culture was removed from the system. The increase in cell density was characterized by $OD_{600} \approx 3.5$ (sample 5× diluted in fresh, sterile LB). Further portions of culture were removed and centrifuged (Sigma 4K15, RCF 5650 g, typically for 20 to 30 min). The resulting supernatant was then passed through a 0.22 μm filter to remove any residual cellular material and the pH was measured (Thermo Orion 410 pH meter), giving a typical pH ≈ 4.3−4.8 due to organic acids generated during fermentation. For comparison, fresh LB has pH ≈ 6.8. At the beginning of the experiment, the cellular material within the 250 mL suspension has a typical dry weight of 8 mg, which by the end of a typical experiment increased to 60 mg, reflecting bacterial growth.

RESULTS AND DISCUSSION

H_2 Production from Anaerobic Batch Cultures with D-Glucose. *E. coli* is able to express four distinct hydrogenases, all of the [NiFe] type and associated with the inner, cytoplasmic membrane of the cell.[28] Hyd-1 and Hyd-2 primarily function as uptake hydrogenases.[30] Hyd-3 is the main H_2 producing hydrogenase. In vivo, it forms part of the membrane-anchored formate hydrogenlyase (FHL) complex, which catalyzes the oxidation of formate to CO_2 and passes the generated reducing equivalents to the [NiFe] active site where proton reduction occurs.[31] Relatively little is known about the fourth hydrogenase Hyd-4, and its physiological role (if any) remains uncertain.[32] For *E. coli* and many other facultative anaerobes, H_2 production is a strictly fermentative process. Expression of all four hydrogenases is strongly repressed by O_2, and the enzymes themselves, with the exception of Hyd-1, are also highly sensitive to even traces of O_2. We followed the aerobic metabolism of *E. coli* growing on rich LB medium supplemented with D-glucose. As expected, the O_2 pressure decreased, while CO_2 increased, but no H_2 production was observed, even when O_2 was exhausted. Clearly, ensuring the system is O_2 free would be critical in large-scale fermentative biohydrogen production. In the absence of O_2 or other suitable external electron acceptors such as nitrate, *E. coli* switches to mixed acid fermentation to derive energy from organic substrates. A mixture of partially oxidized products, CO_2 and H_2 are generated, the exact distribution governed by the carbon source and the intra- and extracellular environment.[33,34] During glucose fermentation, the majority of both CO_2 and H_2 released is generated from oxidation of formate by the FHL complex. To investigate H_2 production, we prepared *E. coli* LB broth cultures supplemented with D-glucose (40 or 100 mM) and purged with N_2 to remove O_2. CERS has the advantage of being sensitive to O_2, enabling us to check the headspace to ensure its absence and continue to purge if traces are still observed. The composition of the gas phase was then measured for up to 5 days by CERS in order to follow the evolution of volatile components. While the short peptides found in LB can be utilized as a sole carbon and nitrogen source for growth, there was no observable H_2 production from cultures grown on nonsupplemented LB.

Figure 3 shows as a typical example the partial pressures of H_2 and CO_2 in the fermentation of 40 mM glucose. The H_2 kinetics has at least three different phases. In the first 2 h, the rise is slow and may give the impression of an induction period; a closer look reveals, however, that H_2 is produced almost

DOI: 10.1021/acs.analchem.6b04924
Anal. Chem. 2017, 89, 2147−2154

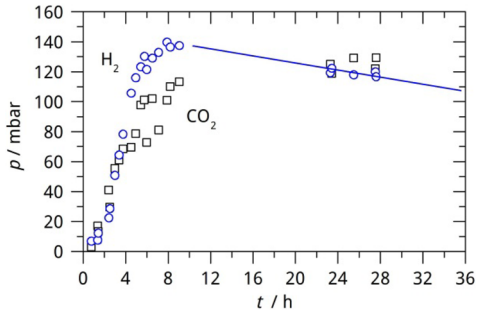

Figure 3. Partial pressures of CO_2 (black, squares) and H_2 (blue, circles) as a function of time, as observed by CERS in the anaerobic fermentation of 40 mM glucose (10 mmol) by *E. coli*. At its peak, 140 mbar of H_2 is produced, equivalent to 7.1 mmol.

immediately, but at a reduced rate. This may reflect differences in H_2 metabolism during different stages of growth, perhaps between the lag and exponential phases. The slow phase is followed by a phase of rapid production peaking around 7 h with a rise half time $t_{1/2}$ of about 1 h. At its peak, 140 mbar of H_2 is produced, equivalent to 7.1 mmol, taking both the solution and headspace into account. With 10 mmol glucose present at the beginning of the experiment, the yield (expressed as mol H_2/mol glucose) is 0.71. After reaching its peak, the H_2 concentration starts to decrease, with an extrapolated half time of about 3−4 days. The CO_2 partial pressure mirrors that of H_2, peaking at 120 mbar (6.9 mmol), although, unlike H_2, no significant decay is apparent. The molar ratio of CO_2/H_2 at its peak is almost equimolar, indicating that the vast majority of hydrogen originates from the oxidation of formate. Similar behavior was observed with 100 mM glucose: in a typical experiment, 363 mbar H_2 was produced, equivalent to 18.5 mmol, and a yield of 0.74, very similar to the lower glucose concentration. However, CO_2 production was proportionally lower than in the 40 mM experiment, with CO_2 peaking around 200 mbar, corresponding to 11.5 mmol and a molar ratio of CO_2/H_2 of only 62%. This might reflect more reducing conditions in the cellular environment, with Hyd-1 or, more likely, Hyd-2 acting as a secondary H_2 producing enzyme in a similar way to cultures grown on glycerol.

For both glucose concentrations, H_2 was observed to decay, while CO_2 remained essentially constant, showing that the cells also exhibit some H_2 uptake. Previous work has shown that deletion of genes encoding uptake hydrogenases can increase the overall yield of H_2.[35,36] Although Hyd-3 has been reported to operate in reverse, coupling H_2 oxidation to CO_2 reduction to formate, this behavior is probably not relevant under physiological conditions.[37] In addition, the absence of any observable CO_2 uptake indicates that the H_2 uptake is primarily due to the respiratory hydrogenases, Hyd-1 and -2, which are not directly coupled to formate dehydrogenase. Hyd-1 primarily couples the oxidation of H_2 to high redox potential electron acceptors, such as O_2, and not to low redox potential acceptors. Since the measurements described here were carried out under strictly fermentative conditions where only low potential electron acceptors such as fumarate are present, it seems more likely that the observed H_2 uptake is due to Hyd-2 activity. This is in agreement with previous work that showed that deletion of Hyd-1 had little effect on H_2 uptake, and a strain carrying deletions in both Hyd-1 and -2 showed no further reduction in H_2 uptake over a strain carrying only a Hyd-2 mutation.[38]

Anaerobic Fermentation of Glycerol by *E. coli*. There is a global oversupply of glycerol due to biodiesel production where transesterification of oils generates glycerol-contaminated aqueous waste.[39] This waste could be a convenient sustainable substrate for organisms such as *E. coli*, which can utilize glycerol for fermentation under certain conditions.[40−42] Its higher degree of reduction could be an advantage compared to sugars; glycerol fermentation typically gives increased yields of more reduced and higher value products for the chemical industry.[43] To investigate H_2 production, we prepared *E. coli* LB broth cultures supplemented with glycerol (80 or 200 mM) and purged with N_2 to remove O_2. Figure 4 shows a typical

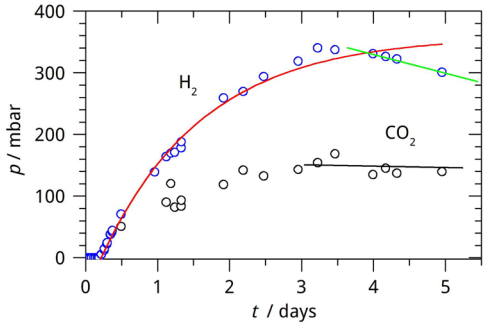

Figure 4. Partial pressures of CO_2 and H_2 as a function of time as observed by CERS in the anaerobic fermentation of 200 mM glycerol by *E. coli*.

example of the evolution of CO_2 and H_2 over 5 days produced by an anaerobic culture supplemented with 200 mM glycerol. The appearance of H_2 is approximately described by exponential growth with half time $t_{1/2}$ = 23 h and an apparent delay of about 6 h (red curve in Figure 4). After reaching its peak at 360 mbar after 3.3 days, the H_2 partial pressure shows a slow exponential decay with half time $t_{1/2}$ = 6.8 d (green curve in Figure 4). The CO_2 pressure broadly mirrors H_2 production, but at 155 mbar, it peaks at a lower value. The lower CO_2/H_2 ratio probably reflects the fact that significant amounts of H_2 are produced by pathways which do not require simultaneous formation of CO_2. This is in agreement with previous work which has shown that Hyd-2 plays also a role in H_2 production during glycerol fermentation, where it acts as a "relief valve" to dispose of excess reducing equivalents.[44,45] For CO_2, no distinct decrease is observed after day 3. The observed decrease in H_2 thus indicates H_2 uptake activity.

Distinctly different behavior is observed for the kinetics of H_2 production depending on the carbon source and its concentration. With 40 mM D-glucose, it has a half time of 1 h, tripling to 3 h for 100 mM, whereas H_2 production is much slower in glycerol, with a half time of 8 h for 98 mM glycerol, increasing to 23 h for 200 mM. For D-glucose, the theoretical maximum fermentation yield (mol H_2 per mol D-glucose) is 2, since up to two formate molecules can be generated from each molecule of glucose via glycolysis and pyruvate cleavage by pyruvate formate-lyase (PFL).[33] For glycerol, the corresponding maximum yield is 1. The observed yields of 0.67−0.74 for D-glucose and 0.27−0.37 for glycerol are within 27−37% of the theoretical maximum yield, remarkably independent of the feed stock or its concentration. The observed yield is only a lower limit which could be improved by extraction of H_2 when formed, thus preventing accumulation and uptake of H_2. Previous work has shown that allowing H_2 build up above

DOI: 10.1021/acs.analchem.6b04924
Anal. Chem. 2017, 89, 2147−2154

glycerol supplemented cultures is detrimental to growth, which would suggest that constantly siphoning off the produced H_2 could be critical for efficient biohydrogen production.[46] The yields are also lower than those obtained from H_2 over-producing mutant strains, which lack uptake hydrogenases and overexpress FHL.[35,36] This reflects the importance of "rewiring" the mixed acid fermentation pathways in order to maximize carbon flow to formate and minimize losses to undesired products such as lactate or succinate. H_2 production is known to be product inhibited; since the experiment was in a sealed system, the buildup of H_2 may have contributed to a reduction in the yield. In addition, Hyd-1 and Hyd-2 primarily operate as H_2 oxidizing enzymes, and they may have contributed to removal of H_2 in the headspace.

Anaerobic Fermentation under a D_2/N_2 Atmosphere. To separate hydrogen generation and consumption, isotopic labeling with deuterium can be used. D_2 labeling of the headspace has previously been employed in combination with membrane inlet mass spectrometry to investigate hydrogenase activity.[47] One disadvantage with this technique is that gas must be constantly sampled from the headspace, limiting the time for which a labeling experiment could be run and also requiring a correction for the depletion of gas in the headspace. Raman spectroscopy has isotopomer selectivity but does not consume any gas. For isotopic labeling of the headspace, we introduced a large excess of D_2 at the beginning of the measurement. Batch cultures of *E. coli* were prepared as before and purged several times to remove any dissolved O_2. A defined mixture of N_2/D_2 was then introduced into the system to a total pressure of 1 bar (typically 600 mbar D_2, 400 mbar N_2).

Figure 5 shows a typical experiment. Although excess hydrogen is known to inhibit certain classes of hydrogenase, there is no delay in the appearance or reduction in the rate of H_2 formation. D_2 consumption has no lag, indicating that the hydrogenases involved in D_2 consumption are already present at the beginning of the measurement. With 40 mM glucose (10 mmol), there are two distinct phases of D_2 consumption which both adopt pseudo first-order behavior; in phase (a), between 0 to 0.5 days, D_2 decays with $t_{1/2}$ = 1.4 d followed by a second phase (b) of slower decay with $t_{1/2}$ = 5.0−5.5 d, which continues up to the end of the measurement (0.5−7 days). No distinct transition in H_2 or CO_2 production is observed between phases (a) and (b). The profiles of H_2 and CO_2 are distinctly different: CO_2 rises to its peak value of about 100 mbar (5.8 mmol) at 3 d, then it remains essentially constant. H_2, however, increases for a longer time, reaching a plateau of 340 mbar (17.3 mmol) after 6−7 days. In the 40 mM glucose experiments with and without D_2, approximately the same amount of CO_2 is produced; it thus seems reasonable to assume that a similar amount of formate is oxidized by the FHL complex, corresponding to around 7.1 mmol H_2. After 7 d, about 350 mbar (17.9 mmol) of D_2 is consumed and an additional 10 mmol more H_2 is produced than would be expected from fermentation alone. This excess can be accounted for if 56% of the D_2 consumed is converted to H_2 through isotope exchange with the solvent. This suggests that some of the consumed D_2 is coupled either directly (through H/D exchange at a hydrogenase active site) or indirectly (perhaps via intermediate electron donation back into the quinone pool) to proton reduction. Such D/H isotope exchange has been well reported in the literature.[47] Rather unusually for such labeling experiments, there is no significant formation of the mixed isotopomer HD; final HD pressures are typically below 15 mbar. In contrast, in previously reported experiments, levels of HD comparable to the added D_2 were observed using isolated hydrogenases, membranes, or cell extracts from a variety of organisms.[47] A similar absence of HD was, however, observed for purified hydrogenases obtained from *Azotobacter vinelandii* and *Ralstonia eutropha* (now *Cupriavidus necator*) when incubated under D_2 in protonated buffer.[48,49]

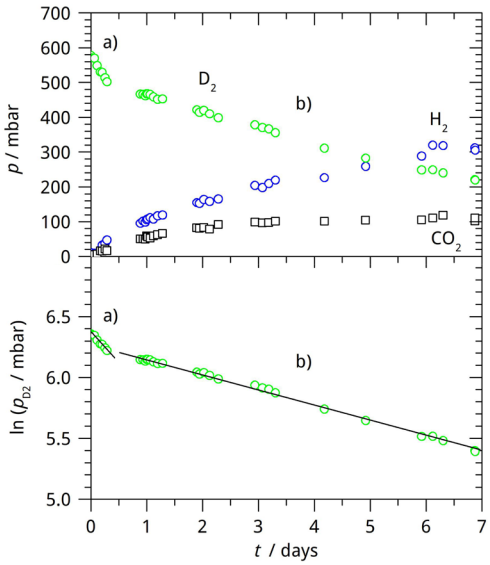

Figure 5. Partial pressures of H_2, D_2, and CO_2 in the anaerobic fermentation of 40 mM glucose under D_2/N_2. The lower plot displays the decay of D_2 on a logarithmic scale, showing two distinct kinetic regimes.

To probe H_2 uptake activity during glycerol fermentation, experiments were performed under an N_2/D_2 atmosphere (typically 600 mbar D_2, 400 mbar N_2, 98 mM glycerol (25 mmol), 3 repeats). Figure 6 shows a typical experiment. Samples consistently show a single phase (labeled "b" in Figure 6), up to day 7, characterized by an exponential decay with $t_{1/2}$ = 5.0−5.7 d, very similar to the phase (b) in glucose-supplemented samples. By day 7, typically around 350 mbar (17.9 mmol) of D_2 is consumed. H_2 continues to rise and appears to start to plateau at a partial pressure of 480 mbar (24.5 mmol) around day 6−7. Unlike glucose fermentation under D_2, CO_2 production does not stop early, but continues to increase, with the profile closely mirroring that of H_2. A similar plateau is observed in CO_2 around day 6−7 with 200 mbar (11.5 mmol) produced, which far exceeds the amount of CO_2 produced in glycerol samples without D_2. As with glucose, no significant formation of HD is observed. Assuming a similar H_2 fermentation yield as in the experiments without D_2, the excess of H_2 produced in phase (b) is of the order of 17−19 mmol; to account for this by D_2 conversion, almost the entire D_2 consumed would have to be converted to H_2, a much higher percentage than in the case of glucose. The assumption of similar fermentation yields would also be at variance with the higher amount of CO_2 produced. The observations that CO_2 production does not stop early but continues rising with H_2, and that more CO_2 is produced indicates a higher fermentation yield of H_2 from glycerol in the presence of D_2, contrary to the behavior in glucose. A significant amount of the excess H_2 is then expected to be due to the increased fermentation, and the

DOI: 10.1021/acs.analchem.6b04924
Anal. Chem. 2017, 89, 2147−2154

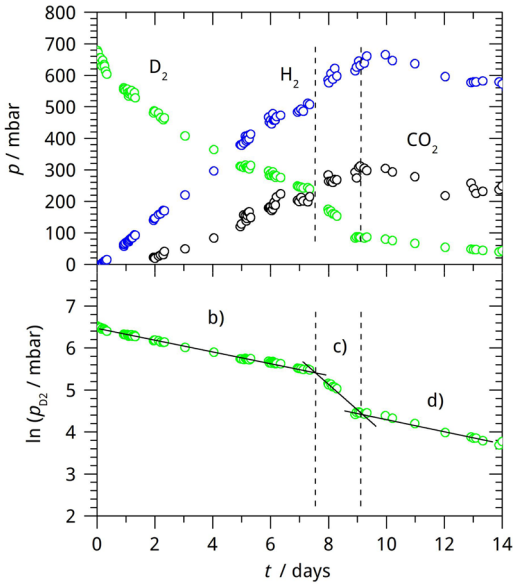

Figure 6. Partial pressures of H_2, D_2, and CO_2 in the anaerobic fermentation of 98 mM glycerol under D_2/N_2. The lower plot displays the decay of D_2 on a logarithmic scale, showing three distinct kinetic regimes.

balance from the conversion of D_2 is then closer to the 56% conversion estimated for glucose. A tentative explanation could be that D_2 triggers more formate production during mixed acid fermentation which is then split into H_2 and CO_2. Clearly more work is required to understand the underpinning mechanisms of this increased fermentation yield. If these mechanisms are better understood, conditions in biohydrogen production from glycerol could possibly be optimized to significantly increase the hydrogen yield.

In all three repeat experiments with glycerol, we observed a single event (labeled "c" in Figure 6) at about day 8−10, just after H_2 and CO_2 appear to plateau and typically lasting for 1 to 2 days. During this event, D_2 consumption significantly increases, with $t_{1/2}$ = 0.8−1.5 d; afterward, it resumes a slower decay as before (labeled "d" in Figure 6). During event (c), 8.4 mmol of D_2 is lost, and 6.6 mmol of H_2 and 5.5 mmol of CO_2 are gained. The sudden change is striking, with accelerated D_2 consumption occurring with increased H_2 and CO_2 production, which suggests that this is not simply D/H exchange. It may reflect increased FHL activity, perhaps due to a sudden surge of formate into the cytoplasm. The phase of rapid D_2 consumption occurs just after H_2 and CO_2 begin to plateau, which may indicate that it coincides with exhaustion of glycerol or some intermediate metabolite. It could also be related to changes in pH or redox potential, as both impact hydrogenase expression and activity. For convenience, all results on glucose and glycerol fermentation under N_2 and N_2/D_2 are summarized in the Supporting Information (SI Tables S2 and S3), including yields and indicating the number of repeat experiments.

Although the precise mechanism of hydrogenase turnover is still debated, a recent high resolution crystallographic study has obtained a structure of a hydride intermediate for a [NiFe] hydrogenase, confirming that H_2 is cleaved and formed heterolytically.[50] A further oxidation step is then required before the hydride can be oxidized and then removed from the active site as a proton. The absence of major HD formation in our measurements could indicate that the second oxidation step is much faster than a recombination of the deuteride intermediate with a solvent-derived proton and release of HD.[47] Alternatively, HD may be formed but recaptured by the same active site (a cage effect mechanism) or it may simply indicate that, at the enzyme concentrations present in culture, any HD will undergo more encounters before being released to the environment as H_2.[51] HD might also have a large kinetic isotope effect favoring uptake over D_2, so that it is preferentially consumed once formed. These mechanistic details of isotope conversion can be resolved in future experiments employing the CERS technique.

CO Blocks Anaerobic Hydrogen Production of *E. coli* with Glycerol. CO is a potent inhibitor of many metalloenzymes, including certain classes of hydrogenases. Many of the O_2 tolerant hydrogenases, such as *E. coli* Hyd-1, are also typically more resistant to CO inhibition, whereas O_2 sensitive hydrogenases, such as *E. coli* Hyd-2 and -3, are inhibited by CO.[30,51−53] To study this effect, we introduced CO into the headspace along with N_2 and D_2 during the purge step. After leaving the culture under the same $CO/D_2/N_2$ atmosphere for a day, the system was purged several times with N_2, and an N_2/D_2 atmosphere was reintroduced into the system. The headspace was then monitored for a further 9 days (see Figure 2). Observed partial pressures of the different components are shown in Figure 7. The presence of CO in the headspace

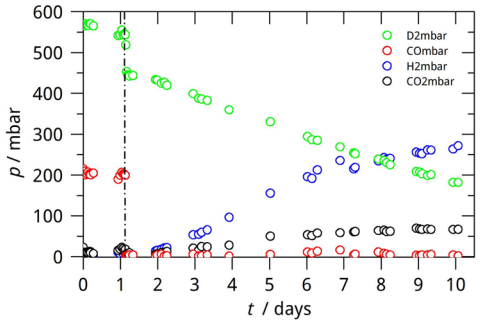

Figure 7. Partial pressures of H_2, D_2, CO_2, and CO in the anaerobic fermentation of 98 mM glycerol. First phase from 0 to 1 d with CO present; second phase from 1 to 10 d where CO has been removed.

completely inhibited formation of H_2 and CO_2 and partially inhibited D_2 uptake. Since Hyd-1 is the only hydrogenase in *E. coli* known to have some level of CO tolerance, we propose that the limited D_2 uptake activity during the first day must be due to Hyd-1. The half-life of 13.6 days for D_2 consumption is considerably longer than in the measurements where CO was not introduced into the headspace. This supports the hypothesis that either or both of Hyd-2 and Hyd-3, which are strongly inhibited under a CO atmosphere, are more important than Hyd-1 under these conditions. A partial recovery of H_2 producing activity is observed when CO is removed. Recovery is not instantaneous, with a delay of around 0.5 days before the onset of D_2 oxidation and 1 day before H_2 production. This may reflect the growth of new cells rather than recovery of cells present during the CO inhibition phase. As in the previous experiments, HD is only formed to a minor extent (see Figure 2). To our knowledge, this is the first demonstration of selective CO inhibition of hydrogenases in *E. coli* whole cells.

DOI: 10.1021/acs.analchem.6b04924
Anal. Chem. 2017, 89, 2147−2154

CONCLUSIONS

Cavity-enhanced Raman spectroscopy (CERS) with optical feedback cw-diode lasers is a sensitive and selective analytical tool for in situ, multicomponent, and isotope selective gas measurements. We have demonstrated the operation with just one Faraday isolator and without active phase and mode matching, greatly simplifying the setup. The improved setup has been employed in its first application to study hydrogen production and consumption by *E. coli*. Under anaerobic conditions, cultures grown on either D-glucose or glycerol produce H_2 and CO_2, simultaneously consuming some of the produced H_2. By introducing D_2, the kinetic processes of hydrogen production and consumption could be separated due to the distinct signatures of each isotopomer. The experiments show that some of the D_2 consumed is converted back to H_2. HD is only formed as a minor component. Different phases with distinctly different kinetic regimes of H_2 and CO_2 production and D_2 consumption were identified. The presence of D_2 seems to increase the H_2 fermentation yield in glycerol. If the mechanisms of this effect are better understood, conditions in biohydrogen production from waste glycerol could be optimized. Although the measurements described here deal with a pure culture, mixed consortia of microorganisms, such as those obtained from biogas slurry, could prove to be a more economical inoculant.[54] In these systems, heat treatment is required in order to remove methanogens, which consume H_2 and generate methane. As previously demonstrated by our group,[22,23] CERS is able to distinguish H_2 and CH_4, so a similar CERS-based approach could be useful for developing and optimizing these systems, confirming the absence of methanogenic organisms by checking the headspace for methane. Due to its unique analytical capabilities, CERS can supplement existing techniques to obtain relevant insights into the biochemistry of the uptake and production of gases and volatile species.

ASSOCIATED CONTENT

Supporting Information

The Supporting Information is available free of charge on the ACS Publications website at DOI: 10.1021/acs.analchem.6b04924.

Table S1, CERS Raman characteristics of compounds measured; Table S2, Yields and kinetics of H_2 production during anaerobic fermentation under an N_2 atmosphere; Table S3, Observed yield and kinetics of H_2 production and D_2 consumption during anaerobic fermentation under an N_2/D_2 atmosphere (PDF).

AUTHOR INFORMATION

Corresponding Author

*E-mail: m.hippler@sheffield.ac.uk.

ORCID

Michael Hippler: 0000-0002-3956-3922

Notes

The authors declare no competing financial interest.

ACKNOWLEDGMENTS

We are very grateful to Profs. R. K. Poole and J. Green (University of Sheffield) for substantial help, support, and advice. This work is funded by the University of Sheffield and the NERC (grant NE/I000844/1) and EPSRC (DTA Ph.D. scholarship to T.W.S.) research councils.

REFERENCES

(1) Hosseini, S. E.; Wahid, M. A. *Renewable Sustainable Energy Rev.* **2016**, *57*, 850−866.
(2) Eberle, U.; Felderhoff, M.; Schüth, F. *Angew. Chem., Int. Ed.* **2009**, *48*, 6608−6630.
(3) Turner, J.; Sverdrup, G.; Mann, M. K.; Maness, P. C.; Kroposki, B.; Ghirardi, M.; Evans, R. J.; Blake, D. *Int. J. Energy Res.* **2008**, *32*, 379−407.
(4) Armaroli, N.; Balzani, V. *Angew. Chem., Int. Ed.* **2007**, *46*, 52−66.
(5) Yasin, N. H. M.; Mumtaz, T.; Hassan, M. A.; Rahman, N. A. *J. Environ. Manage.* **2013**, *130*, 375−385.
(6) Show, K. Y.; Lee, D. J.; Tay, J. H.; Lin, C. Y.; Chang, J. S. *Int. J. Hydrogen Energy* **2012**, *37*, 15616−15631.
(7) Lee, H. S.; Vermaas, W. F. J.; Rittmann, B. E. *Trends Biotechnol.* **2010**, *28*, 262−271.
(8) Gupta, S. K.; Kumari, S.; Reddy, K.; Bux, F. *Environ. Technol.* **2013**, *34*, 1653−1670.
(9) Vazquez, G. D.; Arriaga, G. S.; Mondragón, F. A.; Rodríguez, A. L.; Colunga, L. M. R.; Flores, E. R. *Rev. Environ. Sci. Bio/Technol.* **2008**, *7*, 27−45.
(10) Lubitz, W.; Ogata, H.; Rüdiger, O.; Reijerse, E. *Chem. Rev.* **2014**, *114*, 4081−4148.
(11) Quack, M. *Annu. Rev. Phys. Chem.* **1990**, *41*, 839−874.
(12) Sigrist, M. W. *Air Monitoring by Spectroscopic Techniques; Chemical Analysis Series 127*; Wiley: New York, 1994.
(13) Hippler, M.; Mohr, C.; Keen, K.; McNaghten, E. *J. Chem. Phys.* **2010**, *133*, 044308 (1-8).
(14) Hippler, M.; Miloglyadov, E.; Quack, M.; Seyfang, G. Mass and Isotope-Selective Infrared Spectroscopy. In *Handbook of High-Resolution Spectroscopy*; Quack, M., Merkt, F., Eds.; John Wiley: Chichester, 2011; pp 1069−1118.
(15) Tinajero-Trejo, M.; Rana, N.; Nagel, C.; Jesse, H. E.; Smith, T. W.; Wareham, L. K.; Hippler, M.; Schatzschneider, U.; Poole, R. K. *Antioxid. Redox Signaling* **2016**, *24* (14), 765−780.
(16) Weber, A. High-resolution Raman Spectroscopy of Gases. In *Handbook of High-Resolution Spectroscopy*; Quack, M., Merkt, F., Eds.; John Wiley: Chichester, 2011; pp 1153−1236.
(17) Eichmann, S. C.; Kiefer, J.; Benz, J.; Kempf, T.; Leipertz, A.; Seeger, T. *Meas. Sci. Technol.* **2014**, *25*, 075503.
(18) Lavorel, B.; Millot, G.; Rotger, M.; Rouillé, G.; Berger, H.; Schrötter, H. W. *J. Mol. Struct.* **1992**, *273*, 49−59.
(19) Spencer, C. L.; Watson, V.; Hippler, M. *Analyst* **2012**, *137*, 1384−1388.
(20) Hanf, S.; Keiner, R.; Yan, D.; Popp, J.; Frosch, T. *Anal. Chem.* **2014**, *86*, 5278−5285.
(21) James, T. M.; Rupp, S.; Telle, H. H. *Anal. Methods* **2015**, *7*, 2568−2576.
(22) Salter, R.; Chu, J.; Hippler, M. *Analyst* **2012**, *137*, 4669−4676.
(23) Hippler, M. *Anal. Chem.* **2015**, *87*, 7803−7809.
(24) Keiner, R.; Frosch, T.; Massad, T.; Trumbore, S.; Popp, J. *Analyst* **2014**, *139*, 3879−3884.
(25) Jochum, T.; Michalzik, B.; Bachmann, A.; Popp, J.; Frosch, T. *Analyst* **2015**, *140* (9), 3143−3149.
(26) Colunga, L. M. R.; Rodríguez, A. L. *Rev. Environ. Sci. Bio/Technol.* **2015**, *14*, 123−135.
(27) Maeda, T.; Sanchez-Torres, V.; Wood, T. K. *Microb. Biotechnol.* **2012**, *5*, 214−225.
(28) Sargent, F. The model [NiFe]-hydrogenases of *Escherichia coli*. In *Advances in Microbiol Physiology*; Poole, R. K., Ed.; Elsevier, 2016; Vol. *68*.
(29) www.webbook.nist.gov; accessed 23/3/2016.
(30) Lukey, M. J.; Parkin, A.; Roessler, M. M.; Murphy, B. J.; Harmer, J.; Palmer, T.; Sargent, F.; Armstrong, F. A. *J. Biol. Chem.* **2010**, *285*, 3928−3938.
(31) McDowall, J. S.; Hjersing, M. C.; Palmer, T.; Sargent, F. *FEBS Lett.* **2015**, *589*, 3141−3147.

DOI: 10.1021/acs.analchem.6b04924
Anal. Chem. 2017, 89, 2147−2154

(32) Skibinski, D. A. G.; Golby, P.; Chang, Y. S.; Sargent, F.; Hoffman, R.; Harper, R.; Guest, J. R.; Attwood, M. M.; Berks, B. C.; Andrews, S. C. *J. Bacteriol.* **2002**, *184*, 6642−6653.
(33) Bock, A.; Sawers, G. Fermentation. In *Escherichia coli and Salmonella, Cellular and Molecular Biology*, 2nd ed.; Neidhardt, F. C., Curtiss, R., Ingraham, J. I., Lin, E. C. C., Low, K. B., Magasanik, B., Reznikoff, W., Riley, Schaechter, M., Umbarger, H. E., Eds.; American Society for Microbiology: Washington, D.C., 1996; Chapter 18.
(34) Elsharnouby, O.; Hafez, H.; Nakhla, G.; El Naggar, M. H. *Int. J. Hydrogen Energy* **2013**, *38*, 4945−4966.
(35) Maeda, T.; Sanchez-Torres, V.; Wood, T. K. *Appl. Microbiol. Biotechnol.* **2007**, *77*, 879−890.
(36) Maeda, T.; Sanchez-Torres, V.; Wood, T. K. *Microb. Biotechnol.* **2008**, *1*, 30−39.
(37) Pinske, C.; Sargent, F. *MicrobiologyOpen* **2016**, *5*, 721−737.
(38) Redwood, M. D.; Mikheenko, I. P.; Sargent, F.; Macaskie, L. E. *FEMS Microbiol. Lett.* **2008**, *278*, 48−55.
(39) Dobson, R.; Gray, V.; Rumbold, K. *J. Ind. Microbiol. Biotechnol.* **2012**, *39*, 217−226.
(40) Chaudhary, N.; Ngadi, M. O.; Simpson, B. K.; Kassama, L. S. *Adv. Chem. Eng. Sci.* **2011**, *1*, 83−89.
(41) Trchounian, K.; Trchounian, A. *Renewable Energy* **2015**, *83*, 345−351.
(42) Dharmadi, Y.; Murarka, A.; Gonzalez, R. *Biotechnol. Bioeng.* **2006**, *94*, 821−829.
(43) Clomburg, J. M.; Gonzalez, R. *Trends Biotechnol.* **2013**, *31*, 20−28.
(44) Trchounian, K.; Soboh, B.; Sawers, R. G.; Trchounian, A. *Cell Biochem. Biophys.* **2013**, *66*, 103−108.
(45) Blbulyan, S.; Trchounian, A. *Arch. Biochem. Biophys.* **2015**, *579*, 67−72.
(46) Murarka, A.; Dharmadi, Y.; Yazdani, S. S.; Gonzalez, R. *Appl. Environ. Microbiol.* **2008**, *74*, 1124−1135.
(47) Vignais, P. M. *Coord. Chem. Rev.* **2005**, *249*, 1677−1690.
(48) McTavish, H.; Sayavedra-Soto, L. A.; Arp, D. J. *Biochim. Biophys. Acta, Protein Struct. Mol. Enzymol.* **1996**, *1294*, 183−190.
(49) Bernhard, M.; Buhrke, T.; Bleijlevens, B.; De Lacey, A. L.; Fernandez, V. M.; Albracht, S. P. J.; Friedrich, B. *J. Biol. Chem.* **2001**, *276*, 15592−15597.
(50) Ogata, H.; Nishikawa, K.; Lubitz, W. *Nature* **2015**, *520*, 571−574.
(51) Tamiya, N.; Miller, S. L. *J. Biol. Chem.* **1963**, *238*, 2194−2198.
(52) Vincent, K. A.; Cracknell, J. A.; Lenz, O.; Zebger, I.; Friedrich, B.; Armstrong, F. A. *Proc. Natl. Acad. Sci. U. S. A.* **2005**, *102*, 16951−16954.
(53) McDowall, J. S.; Murphy, B. J.; Haumann, M.; Palmer, T.; Armstrong, F. A.; Sargent, F. *Proc. Natl. Acad. Sci. U. S. A.* **2014**, *111*, E3948−E3956.
(54) Li, C.; Fang, H. H. P. *Crit. Rev. Environ. Sci. Technol.* **2007**, *37*, 1−39.

DOI: 10.1021/acs.analchem.6b04924
Anal. Chem. 2017, 89, 2147−2154